Optimizing the Error Diffusion Filter for Blue Noise Halftoning With Multiscale Error Diffusion

Yik-Hing Fung and Yuk-Hee Chan

***Abstract*— A good halftoning output should bear a blue noise characteristic contributed by isotropically-distributed isolated dots. Multiscale error diffusion (MED) algorithms try to achieve this by exploiting radially symmetric and noncausal error diffusion filters to guarantee spatial homogeneity. In this brief, an optimized diffusion filter is suggested to make the diffusion close to isotropic. When it is used with MED, the resulting output has a nearly ideal blue noise characteristic.**

***Index Terms*— Blue noise, error diffusion, halftoning, multiscale error diffusion (MED), printing.**

I. Introduction

The concept of blue noise halftoning was first introduced in [1] by Ulichney. It says that a good quality halftone image should have a frequency spectrum that only contains high frequency random noise. In particular, for a constant gray-level input, dots appeared in its halftoning output should be isolated and their ideal spatial distribution should be aperiodic, homogeneous and isotropic. Accordingly, the spectral energy of the output should be concentrated above the principal frequency f_B which is defined as a function of input gray level g as

$$f_B(g) = \begin{cases} \sqrt{g}, & \text{for } 0 < g \le 1/2 \\ \sqrt{1-g}, & \text{for } 1/2 < g \le 1 \end{cases} \tag{1}$$

and little energy should be in the frequency band below f_B [1], [2].

A multiscale error diffusion (MED) algorithm referred to as feature-preserving MED (FMED) was proposed in [3] recently and it is found in [4] that it is among the best halftoning algorithms in providing outputs of blue noise characteristics. FMED is a two-step iterative algorithm. At each iteration, it selects a not-yet processed pixel, quantizes its value to either 0 or 1, and diffuses its quantization error to the pixel's neighbors with a noncausal diffusion filter. This process repeats until all pixels are processed.

The default diffusion filter used in FMED is basically a 3×3 noncausal filter defined as $F_{id} = [0.5,\ 1,\ 0.5;\ 1,\ 0,\ 1;\ 0.5,\ 1,\ 0.5]/6$, where the center is the error source. The determination of the filter coefficients is based on the idea that, in an isotropic diffusion process, the intensity at a particular point away from the source is inversely proportional to the square of the distance from the source. As shown in Fig. 1(a), the frequency response of this filter is approximately radially symmetric. It is hence able to provide halftones without directional hysteresis.

However, the diffusion filter used in FMED is still a suboptimal approximation of an isotropic filter. In this brief, we derive an optimized diffusion filter for FMED to further improve FMED's performance in providing blue noise halftoning outputs.

Manuscript received December 10, 2010; revised March 26, 2012; accepted July 21, 2012. Date of publication August 2, 2012; date of current version December 20, 2012. This work was supported by the Research Grants Council of Hong Kong Special Administrative Region (PolyU 5130/09E). The associate editor coordinating the review of this manuscript and approving it for publication was Dr. Farhan A. Baqai.

The authors are with the Department of Electronic and Information Engineering, Center for Multimedia Signal Processing, Hong Kong Polytechnic University, Hong Kong (e-mail: yhfung@eie.polyu.edu.hk; enyhchan@polyu.edu.hk).

Color versions of one or more of the figures in this paper are available online at http://ieeexplore.ieee.org.

Digital Object Identifier 10.1109/TIP.2012.2211370

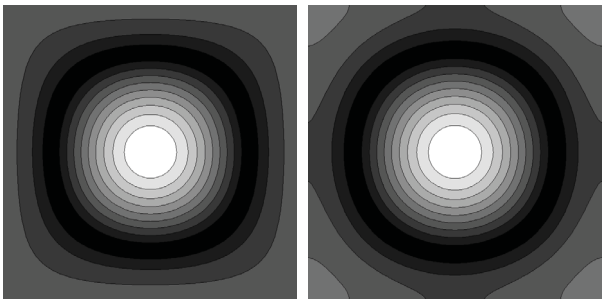

(a) (b)

Fig. 1. Frequency responses of filters (a) F_{id} and (b) $F^o_{(0.7813,0.7813\sqrt{2})}$.

II. Diffusion Filter Optimization

Theoretically, an ideal blue noise halftoning method should produce homogeneously distributed stochastic dither patterns of dots. An isotropic diffusion filter would be necessary to achieve this goal. In practice, a diffusion filter cannot be perfectly isotropic as it has to fit the pixel grid, but it can be optimized to diffuse the quantization error in a close to isotropic manner.

Obviously, in continuous spatial domain, a circular ring-shaped filter defined as

$$F(x,y) = \begin{cases} \frac{1}{((R_2^2 - R_1^2)\pi)}, & \text{if } R_2 \ge \sqrt{x^2+y^2} > R_1 \\ 0, & \text{else} \end{cases} \tag{2}$$

is isotropic, where R_1 and R_2 are, respectively, the inner and the outer radii of the ring, and position $(0, 0)$ is the error source. The error is expelled from the inner circle and equally shared by the region in the ring. Accordingly, the inner circle forms a forbidden region and the ring forms a sharing region. When $R_2 = \sqrt{2}R_1$, we have $R_2^2 = 2R_1^2$ and the two regions have the same area. This also makes the optimization problem become 1-D such that it can be solved more easily.

As an approximation to this circular ring-shaped filter in discrete spatial domain, a desirable diffusion filter, which is referred to as $F^o_{(R_1,R_2)}$ hereafter, can be defined on the basis of the coverage area of the circular ring in a pixel's grid cell. Specifically, its filter coefficient is given by

$$f^o(m,n) = \frac{A(m,n,R_2) - A(m,n,R_1)}{\left(R_2^2 - R_1^2\right)\pi} \tag{3}$$

where (m, n) are the horizontal and vertical offsets from the error source in terms of number of pixels and $A(m, n, R_k)$ for $R_k = R_1, R_2$ is the area covered by circle $\sqrt{x^2+y^2} \le R_k$ in pixel (m, n). Effectively, the filter coefficient for a pixel which is (m, n) pixels away from the point source at the center of pixel $(0, 0)$ is the area covered by the circular ring $R_2 \ge \sqrt{x^2+y^2} > R_1$ in the grid cell associated with that pixel. As we deliberately select $R_2 = \sqrt{2}R_1$, we can adjust one single parameter R_1 to maximize the closeness of $F^o_{(R_1,\sqrt{2}R_1)}$ to an isotropic filter.

In theory, when a filter is isotropic, in its frequency response the magnitude variance of the frequency components covered in an annular ring of any radius should be zero as long as the ring width is sufficiently small. Accordingly, one can define an objective function as

$$J = \sum_{r=0}^{\sqrt{2}\pi} \sigma^2_{f,R_1}(r) \tag{4}$$

where $\sigma^2_{f,R_1}(r)$ is the magnitude variance of the frequency components covered in an annular ring of radius r and width Δ_r

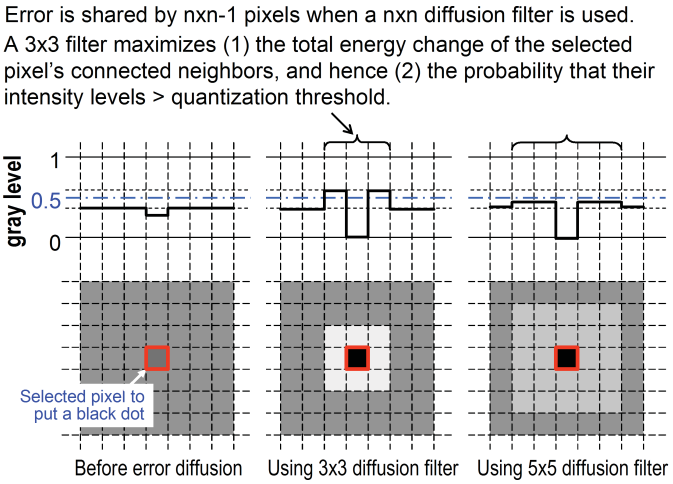

Fig. 2. 3×3 diffusion filter helps to produce isolated dots by maximizing the energy diffused to the connected neighbors of a dot.

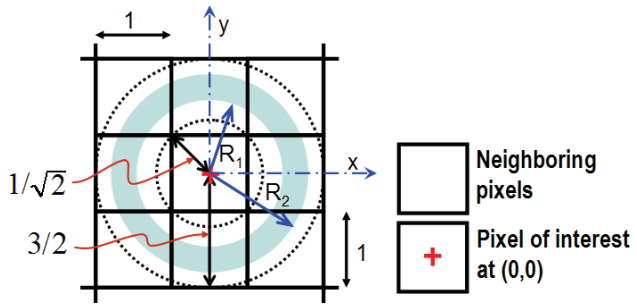

Fig. 3. 3×3 local spatial region for studying the parameter constraint of filter $F^o_{(R_1,\sqrt{2}R_1)}$ for blue noise halftoning.

in the frequency response of filter $F^o_{(R_1,\sqrt{2}R_1)}$, and search for an appropriate R_1 to minimize J under some predefined constraints.

In blue noise halftoning, formation of isolated dots instead of clusters in the output should be encouraged. To achieve this, a 3×3 diffusion filter should be used as it can maximize the amount of error diffused from the central pixel to its 8 connected neighbors as shown in Fig. 2. If the central pixel is assigned a black dot, it will be more likely for us to assign white dots to its connected neighbors in the future. Accordingly, isolated black dots will be more likely to occur. In contrary, when the central pixel is assigned a white dot, it is more likely to be surrounded by black dots at the end.

Fig. 3 shows a 3×3 local spatial region whose central pixel is a quantization error source. Let the center of the central pixel be the origin of a continuous reference x-y coordinate system. The area covered by circular ring $R_2 = \sqrt{2}R_1 \geq \sqrt{x^2+y^2} > R_1$ in a particular pixel grid determines the corresponding coefficient of filter $F^o_{(R_1,\sqrt{2}R_1)}$ for that pixel. In practice, $f^o(0,0)$, the $(0,0)^{\text{th}}$ coefficient of filter $F^o_{(R_1,\sqrt{2}R_1)}$, must be zero as all error must be diffused away from the source pixel. This implies $R_1 \geq 1/\sqrt{2}$. The upper bound of R_1 is $R_1 \leq 3/2\sqrt{2}$ as $R_2 = \sqrt{2}R_1 \leq 3/2$ must be held to confine the size of $F^o_{(R_1,\sqrt{2}R_1)}$ to be 3×3.

The optimal R_1 should hence be searched in the range of $1/\sqrt{2} \leq R_1 \leq 3/2\sqrt{2}$ to minimize objective function (4). Fig. 4 shows our searching result. It can be found that J is minimum at $R_1 = 0.7813$. The corresponding filter is then given as

$$F^o_{(0.7813,0.7813\sqrt{2})} = \begin{bmatrix} 0.0717 & 0.1783 & 0.0717 \\ 0.1783 & \underline{0} & 0.1783 \\ 0.0717 & 0.1783 & 0.0717 \end{bmatrix}. \quad (5)$$

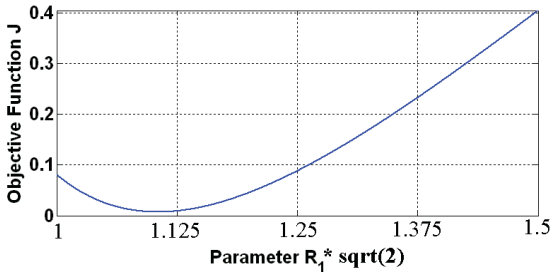

Fig. 4. Plot of J versus $\sqrt{2}R_1$.

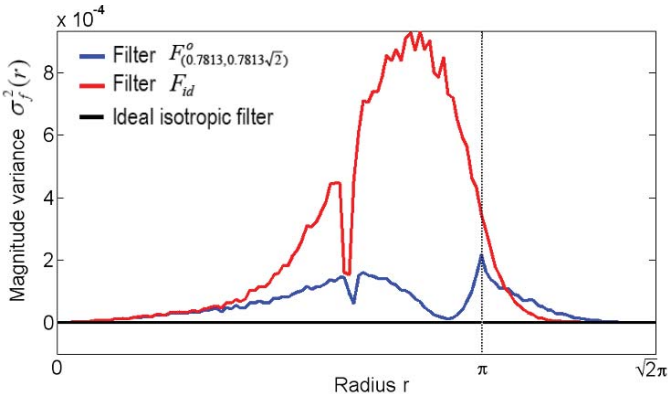

Fig. 5. Magnitude variance of the frequency components covered in an annular ring of radius r in the frequency response of a diffusion filter.

Fig. 1 shows the contour plots of the frequency responses of filters F_{id} and $F^o_{(0.7813,0.7813\sqrt{2})}$ for comparison. Fig. 5 shows the magnitude variance of the frequency components covered in an annular ring of width $\Delta_r = \sqrt{2}\pi/128$ in their frequency responses. One can see that the performance of $F^o_{(0.7813,0.7813\sqrt{2})}$ is closer to the ideal isotropic filter as compared with F_{id}. In other words, error can be diffused to all directions more evenly with $F^o_{(0.7813,0.7813\sqrt{2})}$. This is expected as $F^o_{(0.7813,0.7813\sqrt{2})}$ is optimized to provide a close to isotropic performance.

III. FMED With the Optimized Filter

Without loss of generality, consider we want to halftone an input gray-level image $\mathbf{X}$ of size $2^l \times 2^l$, where l is a positive integer, to obtain an output binary image $\mathbf{B}$. The values of $\mathbf{X}$ are within 0 and 1.

FMED is a two-step iterative algorithm. At the beginning, an error image $\mathbf{E}$ is initialized to be the gray-level input image $\mathbf{X}$. Pixels of $\mathbf{B}$ are then picked one by one iteratively to determine their intensity values until a termination criterion is satisfied. For reference purpose, the intensity values of pixels (m,n) of $\mathbf{X}$, $\mathbf{E}$ and $\mathbf{B}$ are, respectively, denoted as $x_{m,n}$, $e_{m,n}$ and $b_{m,n}$.

In the first step of each iteration cycle, a pixel in $\mathbf{B}$ is selected via the "extreme error intensity guidance" based on the most updated $\mathbf{E}$. Readers who are interested in the operation of extreme error intensity guidance may refer to [3] for the details. Let the coordinates of the selected pixel be (i,j). A dot is then introduced to pixel (i,j) of $\mathbf{B}$ in the second step by assigning a corresponding value (0 or 1) to $b_{i,j}$, and the error image $\mathbf{E}$ is updated by diffusing the error $(= b_{i,j} - e_{i,j})$ to pixel (i,j)'s neighbors in $\mathbf{E}$ with the optimized

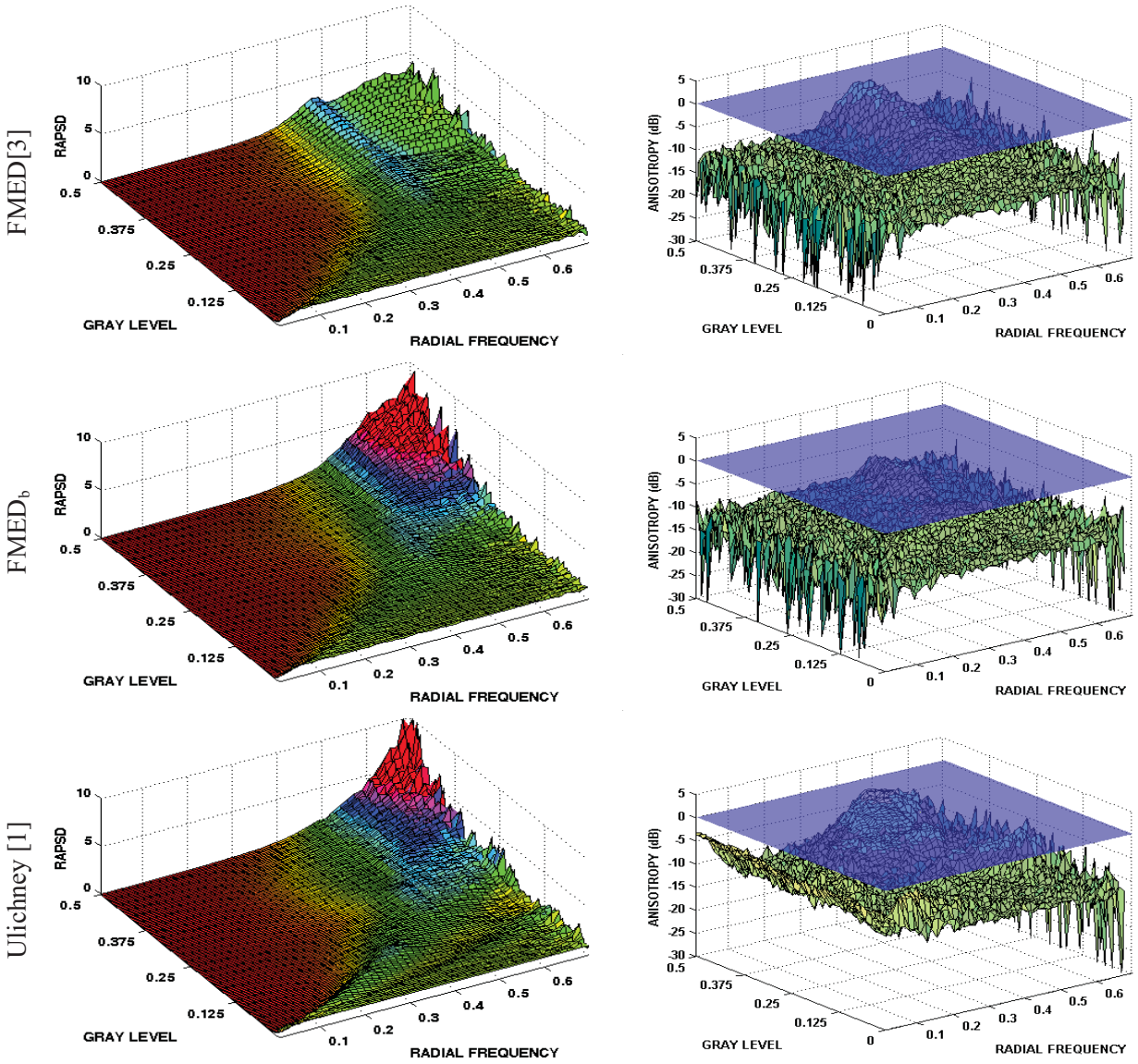

Fig. 6. (a) RAPSD and (b) anisotropy of evaluated algorithms.

diffusion filter $F^o_{(0.7813,0.7813\sqrt{2})}$ as

$$e_{m,n} = \begin{cases} 0, & \text{if } (m,n) = (i,j) \\ e_{m,n} - f^o(m-i, n-j) & \text{if } (m-i, n-j) \\ \quad \cdot d_{m,n} \cdot (b_{i,j} - e_{i,j})/s, & \in \Omega \backslash \{(0,0)\} \end{cases} \tag{6}$$

where Ω is the filter support of $F^o_{(0.7813,0.7813\sqrt{2})}$

$$d_{m,n} = \begin{cases} 0, & \text{if } b_{m,n} \text{ has been assigned a value} \\ 1, & \text{else} \end{cases} \tag{7}$$

and

$$s = \sum_{(m-i,n-j)\in\Omega} f^o(m-i, n-j) \cdot d_{m,n}. \tag{8}$$

In the case when $s = 0$, we exploit a filter with a larger support window to allow the algorithm to proceed. Specifically, starting from $R_2 = 0.7813\sqrt{2}$, we gradually increase the value of R_2 by 0.5 until $s \neq 0$.

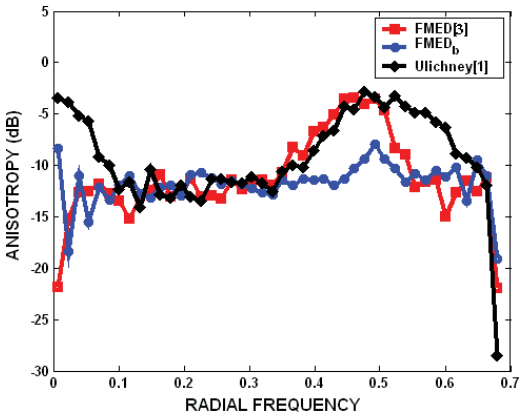

Fig. 7. Anisotropy performance of various algorithms at gray level 0.5.

These two steps are repeated until the sum of all pixels of **E** is bounded in absolute value by 0.5. Note that the total number of iterations is bounded by the total number of pixels in the input image.

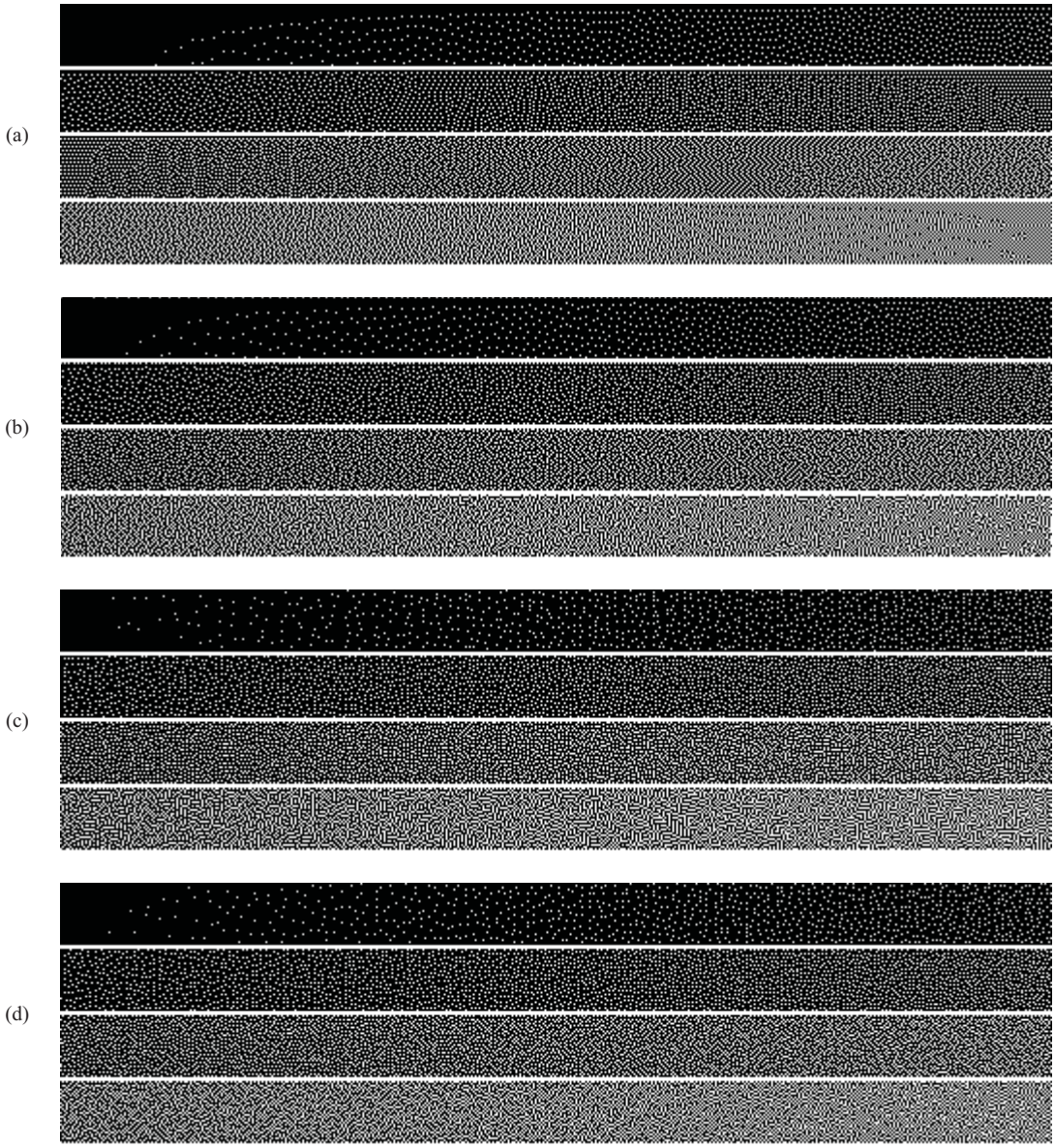

Fig. 8. Halftoning results of a gray ramp image. (a) $\text{SED}_{\text{serpentinescan}}$ [6]. (b) Ulichney [1]. (c) FMED [3]. (d) FMED_b.

For reference propose, the FMED that works with the optimized default diffusion filter as presented in this section is referred to as FMED_b hereafter.

IV. Performance Analysis

A simulation was carried out to investigate the improvement that the proposed filter can achieve. Ulichney's algorithm [1] is a conventional blue noise halftoning algorithm and, as a reference, it was also evaluated for comparison. As for other state-of-the-art halftoning methods, their evaluation results are not included in this brief due to the page constraint. One can refer to [4] and other reported literature such as [5] for comparison. The evaluated algorithms were applied to a set of constant gray-level images of size 256×256 and the dot distributions of their outputs were studied in terms of Radially averaged power spectrum density (RAPSD) and Anisotropy. RAPSD and anisotropy are two measures defined in [1] to analyze the spectral characteristics of a halftone pattern [1].

In terms of RAPSD, the improvement of FMED_b over FMED is obvious as shown in Fig. 6(a). There is a ridge in FMED's RAPSD surface around radial frequency 0.46 when gray level $g > 0.25$, which marks the fundamental frequency of a weak pattern noise in the output halftones. In contrast, FMED_b's RAPSD is globally smooth. The high energy region and the low energy region are well separated. Another observation is that FMED_b's surface is flat in high energy region for small g and generally has no ripple over the surface while there is a ripple in Ulichney's surface when $g < 0.125$. Note that multiple humps or peaks in the power spectrum of a halftone imply the existence of pattern noise in the halftone. From that point of view, FMED_b's output is free from any pattern noise.

Anisotropy is used to measure the strength of directional artifact. As shown in Fig. 6(b), though the anisotropy values of all algorithms are well below zero for all g, the anisotropy surface of FMED_b is globally flatter than FMED's and Ulichney's. This implies that the spatial distribution of the minority dots in FMED_b's outputs is closer to isotropic at all input gray levels and the performance is consistent for all gray level g. As an example for

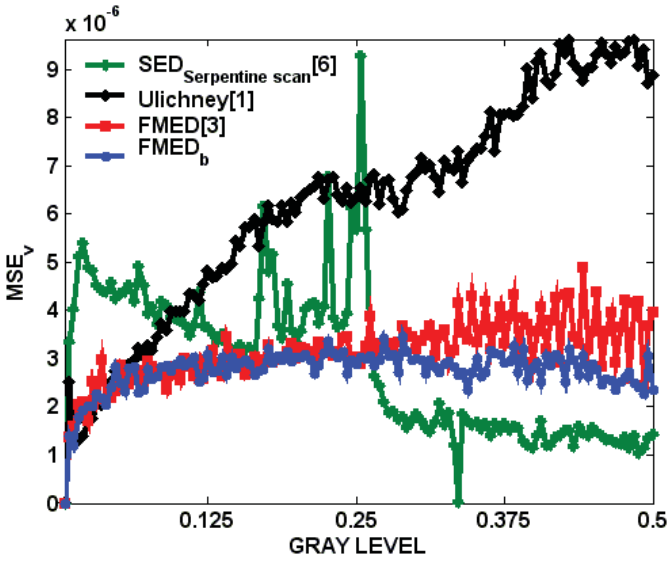

Fig. 9. MSE_v performance of various algorithms.

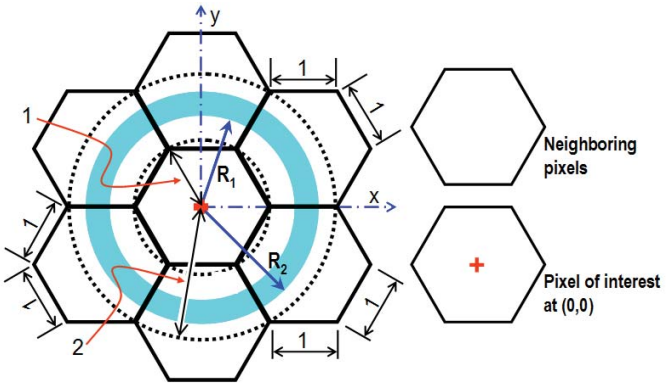

Fig. 10. Local spatial region in a hexagonal grid for studying the parameter constraint of a diffusion filter.

easier comparison, Fig. 7 shows their anisotropy performance at gray level 0.5.

As a matter of fact, since the diffusion filter used in FMED_b is an optimized approximation of a noncausal circular ring-shaped filter, the dot distribution at its halftone output is close to isotropic. The imperfection is solely due to the unavoidable grid constraint.

Fig. 8 shows the halftoning results of a ramp image obtained with various algorithms for subjective evaluation. The ramp covers the range of gray levels from 0 to 0.5 only as the outputs for the range from 0.5 to 1 can be obtained by changing the roles of black and white dots.

Fig. 9 shows the MSE_v performance of various algorithms. In particular, MSE_v is defined as

$$\text{MSE}_v = \frac{1}{2^l \times 2^l} \left\| \text{hvs}(\mathbf{X}, \text{vd}, \text{dpi}) - \text{hvs}(\mathbf{B}, \text{vd}, \text{dpi}) \right\|^2 \qquad (9)$$

where hvs is the HVS filter function defined in [5], vd is the viewing distance in inches and dpi is the printer resolution. In Fig. 9, a viewing distance of 40 inches and a printer resolution of 1000 dpi were considered. FMED_b provides a consistent, flat performance and it is better than [1] and [3]. Apparently, [6] can provide a better performance than FMED_b when $0.75 > g > 0.25$. However, by inspecting Fig 8(a), one can see noise of regular patterns in several large regions in the midtones. Its real performance is actually inferior to FMED_b. In fact, an intensive study on the performance of [6] was reported in [4] and it was found that its RAPSD and anisotropy performance are even inferior to those of [3].

V. Conclusion

In this brief, we derived an optimized error diffusion filter for FMED [3] to achieve blue noise halftoning. This noncausal diffusion filter was optimized such that the diffusion is as close to isotropic as possible. When FMED works with the optimized filter, it is able to eliminate directional hysteresis, distribute dots aperiodically and homogenously, and provide outputs bearing the desirable blue noise characteristics.

In [7], Stevenson and Arce extended the idea of error diffusion to handle hexagonally sampled images and showed that better image quality can be obtained by hexagonal halftoning. Though the filter proposed in this brief was designed based on the assumption that the processing image was sampled in a rectangular grid, the idea can be easily extended to design a filter for images sampled in a hexagonal grid.

As shown in Fig. 10, to expel all energy from the central pixel and maximize the energy diffused to the central pixel's six connected neighbors, the circular ring associated with filter $F^o_{(R_1,R_2)}$ should be bounded by $R_1 \geq 1$ and $R_2 = \sqrt{2}R_1 \leq 2$. Hence, the optimal filter for an image sampled in a hexagonal grid can be obtained by searching the optimal R_1 in the range of $1 \leq R_1 \leq \sqrt{2}$ to minimize objective function (4).

Green noise halftoning is desirable when handling nonideal printing conditions. Some pioneer works on this area can be found in [8] and [9]. While the concern of this brief is on blue noise halftoning, its extension to account for green noise is also possible. Theoretically, in green noise halftoning we should encourage formation of dot clusters instead of isolated dots, and hence the lower bound of R_1 should be increased as compared with the case of blue noise halftoning. Accordingly, we should define another range of potential R_1 values and search its optimal value to minimize objective function (4). This will be studied in our next work.

References

[1] R. A. Ulichney, "Dithering with blue noise," *Proc. IEEE*, vol. 76, no. 1, pp. 56–79, Jan. 1988.

[2] D. L. Lau, R. A. Ulichney, and G. R. Arce, "Blue and green noise halftoning models," *IEEE Signal Process. Mag.*, vol. 20, no. 4, pp. 28–38, Jul. 2003.

[3] Y. H. Chan and S. M. Cheung, "Feature-preserving multiscale error diffusion for digital halftoning," *J. Electron. Imag.*, vol. 13, no. 3, pp. 639–645, 2004.

[4] Y. H. Fung, K. C. Lui, and Y. H. Chan, "A low-complexity high-performance multiscale error diffusion technique for digital halftoning," *J. Electron. Imag.*, vol. 16, no. 1, pp. 1–12, 2007.

[5] D. L. Lau and G. R. Arce, *Modern Digital Halftoning*, 2nd ed. Boca Raton, FL: CRC Press, 2008.

[6] R. W. Floyd and L. Steinberg, "An adaptive algorithm for spatial gray scale," in *SID Int. Symp. Dig. Tech. Papers*, 1975, pp. 75–77.

[7] R. L. Stevenson and G. R. Arce, "Binary display of hexagonally sampled continuous-tone images," *J. Opt. Soc. Amer.*, vol. 2, no. 7, pp. 1009–1013, 1985.

[8] D. L. Lau, G. R. Arce, and N. C. Gallagher, "Green-noise digital halftoning," *Proc. IEEE*, vol. 86, no. 12, pp. 2424–2442, Dec. 1998.

[9] D. L. Lau, G. R. Arce, and N. C. Gallagher, "Digital color halftoning with generalized error diffusion and multichannel green-noise masks," *IEEE Trans. Image Process.*, vol. 9, no. 5, pp. 923–935, May 2000.